ANL/CHM/CP-97337 Proc., Intl. Workshop on Electron Correlations & Materials Properties, Crete, Greece - June 28-July 3, 1998 Plenum Press Publ.

THE ROLE OF SELECTED f IONS IN THE SUPPRESSION OF HIGH-T_C SUPERCONDUCTIVITY

L. Soderholm[1] and U. Staub[2]

[1]Chemistry Division, Argonne National Laboratory, Argonne IL 60439, USA
[2]Swiss Light Source, CH-5232 Villigen PSI, Switzerland

INTRODUCTION

The initial observations of superconductivity at temperature above 77K in copper-oxide based materials was surprising from a variety of different perspectives. Among the unexpected findings were reports of superconductivity for the series $RBa_2Cu_3O_7$ where R is a rare earth (Y, Nd-Tm)[1,2], which may carry a large, local magnetic moment. Superconductivity was subsequently demonstrated for all 4f analogs in this series except Ce, Pr, and Tb. In addition to the $RBa_2Cu_3O_7$ series, there are several other CuO based series of superconductors that are formed by substituting R ions. The most studied of these are listed in Table I, together with the f ions that form isostructural compounds and their superconducting critical temperatures (T_c). The presence of an R ion with a large magnetic moment does not significantly influence the superconductivity. In contrast, even the presence of small concentrations of magnetic impurity ions in a conventional superconductor inhibits superconductivity by interfering with the formation of Cooper pairs.

Most R ions substitute into an isostructural series with no observable effect on the superconducting properties of the material. As can be seen from Table I, there are notable exceptions to this observation. In particular, the rare-earth ions Ce, Pr, and Tb, together with the 5f-actinide ions Am and Cm, sometimes behave anomalously. These ions either do not form an isostructural phase, or if the phase forms it may not be superconducting. The fact that an f-ion can suppress superconductivity is clearly demonstrated in the isostructural series $Y_{1-x}Pr_xBa_2Cu_3O_7$ ($0<x<1$)[3], in which the critical temperature decreases with increasing x, such that for concentrations of Pr greater than $x\approx0.5$, the samples no longer superconduct.

DISCLAIMER

There have been at least four mechanisms proposed to account for the suppression of superconductivity by selected f ions: (1) Hole filling. The suppression of T_c in the $RBa_2Cu_3O_7$ series was initially attributed to the presence of a tetravalent ion at the R site that would effectively transfer charge density according to:

$$R^{3+}Ba_2Cu_2^{2+}Cu^{3+}O_7 \rightarrow R^{4+}Ba_2Cu_3^{2+}O_7,$$

thereby filling the holes on the CuO planes that are responsible for superconductivity. Whereas this mechanism does not play a significant role in the T_c suppression observed in $PrBa_2Cu_3O_7$, it has been subsequently used to understand other Ce and Am compounds. (2) Hole localization, (3) Hybridization of 4f with oxygen 2p orbitals. The latter two mechanism are sometime combined[4,5], and (4) Magnetic-pair breaking[6]. Whereas each of these theories can explain some aspects of the available data, a comprehensive understanding of T_c suppression by selected f ions has yet to emerge.

The ability of select f-ions to sometimes suppress superconductivity is the subject of this article. In an effort to clearly delineate the effects of R substitution on T_c, we have undertaken a systematic study of f-ion substitutions into three different high-T_c series, $RBa_2Cu_3O_7$, R_2CuO_4 and $Pb_2Sr_2RCu_3O_8$. Herein we present a summary of our results. We focus the discussion on results from the R ions that have shown to behave anomalously, that is Ce, Pr, Tb, Am and Cm. A more general review of the overall aspects of our work is presented elsewhere [7]. We begin by reviewing relevant chemical and electronic properties of these f-ions, then we present results from the relevant analogs of the three systems that we studied, and follow these results this with a discussion of the systematics that have emerged from this study.

CHEMICAL AND ELECTRONIC PROPERTIES OF f-IONS

The f-ion has three characteristics of importance relative to it's influence on superconductivity in high-T_c oxides: (1) the chemical behaviour of the ions, which includes ion size and valence stabilities, (2) electronic behaviour, including both single ion and bonding properties and (3) the single-ion and collective magnetic properties. These will be discussed in turn.

The rare-earth ions, excluding Y, La and Lu, have partially filled 4f-states. The f-orbitals are not effectively screened from the nucleus, therefore their ionic radii decrease across the lanthanide series, as shown in Table II. This decreasing size with increasing atomic number, the lanthanide contraction, effectively buries the valence f-orbitals in the s-, p-, and d-electron density. As a result, the f-electrons are localized, and the f-orbitals are not readily available for bonding or interactions with surrounding near-neighbour ions. Their electronic properties are predominantly influenced by electrostatic interactions and they can be treated within single-ion models. Ce^{3+} has the most exposed f-orbitals, which are thought to sometimes hybridize with ligand orbitals resulting in novel electronic properties, including heavy-fermion behaviour and the Kondo effect[8,9]. The ions heavier than Nd are generally considered to behave as trivalent ionic spacers, and the f-states are often treated theoretically as core states. For the most part, the chemistry of these elements is determined by the size of the ion.

Table I. Superconducting CuO series based on R substitutions. Single phase isostructural compounds form except where listed as a parenthetical exception, in which case isostructural member does not form.

Series	R	Exceptions	Approx. T_c (K)
$RBa_2Cu_3O_7$	Y, La-Yb, Cm	(Ce), Pr, (Tb)	92
$RBa_2Cu_4O_8$	Nd-Er	(Tb)	51-84
$R_{1.85}M_{.15}CuO_4$	Pr-Eu, Cm; M=Ce^{4+},Th^{4+}	Cm	24
$Pb_2Sr_2R_{.5}Ca_{.5}Cu_3O_8$	La-Tm, Am, Cm	Ce, Am, Cm	<84
$Bi_2Sr_2R_{.5}Ca_{.5}Cu_2O_8$	Y, Nd-Tm		<85
$(R_{1.5}Ce_{.5})Sr_2Cu_2NbO_{10}$	Pr-Eu	Pr	51-84

Table II. The standard electrode potentials, E^0, for the reduction of the tetravalent to the trivalent valence state[10]. The higher the number, the more stable the trivalent relative to the tetravalent state. Also listed are the trivalent ionic radii for a variety of lanthanide[11] and actinide[12] ions.

4f Element	Radius 3+ (A)	Reduction Potential (eV)	5f Element	Radius 3+ (A)	Reduction Potential (eV)
La	1.160				
Ce	1.143	1.7			
Pr	1.126	3.1			
Nd	1.109	5.0	U		-0.52
			Np		0.15
Sm	1.079		Pu		1.0
Eu	1.066		Am	1.11	2.4
Gd	1.053		Cm	1.10	3.2
Tb	1.040	3.2	Bk	1.08	1.7
Dy	1.027	5.2	Cf	1.08	3.2
(Y)	1.019				
Ho	1.015				
Er	1.004				

Whereas the predominant oxidation state of the lanthanide series is trivalent, selected f-ions are redox active under favourable conditions. Ce, Pr and Tb have energetically accessible tetravalent states in oxidic systems. Ce is the most easily oxidized with a comparatively stable 4+, tetravalent state. A variety of complex oxides containing Ce^{4+} are known[13]. Pr and Tb also form complex oxide compounds in their tetravalent states, the latter of which is isoelectronic with Gd^{3+}, and has a half-filled f shell. The relative stabilities of the tetravalent states of lanthanides are compared in Table II. These data are obtained electrochemically in non-complexing solutions. We argue that although the exact reduction potentials may not be valid in our complex oxides, the trends established by these data are followed. In other words, within an isostructural series, Ce is the most likely to be tetravalent, with Pr and Tb exhibiting similar behaviour.

The actinide series is the 5f counterpart of the lanthanides series, with partially filled 5f states. Whereas an actinide contraction exists across this series for the same reasons as the lanthanide contraction, the effect is not as important. The 5f orbitals are not as buried in the core-electron density. This is demonstrated by the comparison of Pr^{3+} ($4f^2$) with Cm^{3+} ($5f^7$) shown in Figure 1. It is clear that although the ionic radius of Cm^{3+} is slightly smaller than that of Pr^{3+}, the 5f valence orbitals on Cm extend radially further from the nucleus than do their 4f counterparts. The result is that Cm^{3+} and Am^{3+} are expected to have valence f orbitals that are more influenced than the 4f ions by their surrounding ligands. The 5f orbitals are more able to hybridize effectively with ligand orbitals than the valence 4f orbitals in the lanthanide series.

The chemistry of the actinide elements is much more complex than that of the lanthanides[10]. The lighter actinides have multiple oxidation states accessible in both solution and in the solid state. Whereas stable trivalent and tetravalent states are reported for all the ions from Th-Bk in solid oxides, Am and Cm are the only two ions that are expected to form isostructural members of a R-CuO series. Elements lighter than Am are expected to reduce Cu during synthesis, and therefore not form the desired compounds. Higher Z elements are expected to show effects of radiation damage that vitiate property characterization.

Figure 1 The radial distribution of the f-electron density of Pr^{3+} ($4f^2$) is compared with that of Cm^{3+} ($4f^7$). The vertical lines at 1.10 and 1.226 Å represent the ionic radii of Cm and Pr respectively (see Table II)

RESULTS

$RBa_2Cu_3O_7$

This series has been extensively studied. The substitution of R results in isostructural compounds for R=Y, La-Yb (except Ce,Pr, Tb) and Cm. The Ce and Tb analogs do not form single-phase materials, and studies of substitutions into bulk $YBa_2Cu_3O_7$ show very limited stability ranges for both ions. The range of phase stabilities of Ce and Tb in $R_{1-x}Y_xBa_2Cu_3O_7$ increase when samples are made as thin films, into which it is possible to substitute to concentrations of $x < 0.3$ for Ce and $x < 0.7$ for Tb [14]. Resistivity data from these thin films show that T_c is suppressed with increasing x for both Ce and Pr, whereas T_c remains constant with x for the Tb samples through the substitutional range. These data are summarized in Figure 2.

Figure 2. The resistivity of $R_{1-x}Y_xBa_2Cu_3O_7$ thin films as a function of x for R = Ce, Pr and Tb[14]. Circles represent Ce data, squares Pr data and triangles Tb data. Data available over range of phase stability.

Very little work has been done on $Ce_{1-x}Y_xBa_2Cu_3O_7$. Attempts to prepare samples even at low doping levels results in the production of $BaCeO_3$, a stable perovskite phase that forms easily under the synthetic conditions required to form the superconductor. The work on thin film samples [14] provides evidence of T_c suppression, but there is little characterization on the oxidation state of Ce in this sample. Bulk samples of $Ce_{.2}Y_{.8}Ba_2Cu_3O_7$ have been studied using x-ray absorption near-edge structure (XANES)[15] spectroscopy, and have been shown to contain primarily Ce^{4+}. Further work to characterize Ce in this series would be useful.

A variety of experiments have been centered on the Tb oxidation state and hybridization in $Tb_{1-x}Y_xBa_2Cu_3O_7$ [16,17]. An analysis of neutron diffraction data on a x=0.1 sample reveals that Tb is incorporated into the sample, substituting at the Y site. There are no anomalies observed in the lattice constants or in the planar-oxygen thermal parameters determined from the neutron data. This result would be expected if Tb is trivalent because

their Y^{3+} and Tb^{3+} have very similar ionic radii, as shown in Table II. However the low concentration prohibits the determination of a Tb oxidation state from Tb-O distances alone. Paramagnetic susceptibility data also suggest that Tb is trivalent. An effective moment of $\mu_{eff}=(9.8\pm0.3)\mu_B$ was determined by fitting experimental data. This measured moment compares with free-ion effective moments of $9.72\mu_B$ and $7.94\ \mu_B$ for the Tb^{3+} and Tb^{4+} respectively. Further support for trivalent Tb in this material is obtained from a calculation of the single-ion paramagnetic susceptibility for comparison with experiment. Assuming a sublattice of non-interacting Tb ions with a valence of 3+ and no significant hybridization, the effect of the crystal-field generated by the ions surrounding the Tb was modeled using crystal-field parameters interpolated from other $RBa_2Cu_3O_7$ compounds [17]. Including J-mixing and intermediate coupling effects, the single-ion susceptibilities were calculated as a function of temperature, and agree very well with the measured values. For comparison, Tb^{4+} has a spherically symmetric $^8S_{7/2}$ ground term that is not affected to first order by the crystal field, and therefore the free ion susceptibility is the best value to compare with experiment. It is clear that the magnetic data favor model in which Tb is trivalent in $Tb_{1-x}Y_xBa_2Cu_3O_7$. This result is further confirmed by the x-ray absorption near-edge (XANES) data shown in Figure 3. A comparison of the Tb L_3-edge data from $Tb_{1-x}Y_xBa_2Cu_3O_7$ with appropriate trivalent and tetravalent standards demonstrates that Tb is essentially trivalent when substituting for Y in this structure, confirming the analysis of the diffraction and the magnetic susceptibility results.

Figure 3. Tb L_3-edge x-ray absorption data from $Tb_{1-x}Y_xBa_2Cu_3O_7$ (solid line) are compared with a Tb^{3+} standard, $TbCl_3$, and a Tb^{4+} standard, $SrTbO_3$. These data were obtained through electron-yield detection at ambient temperature [17].

The incorporation of increasing amounts of Tb into $Y_{1-x}Tb_xCu_3O_7$ does not influence the superconducting properties of the material. The suppressed T_c previously reported for $TbBa_2Cu_3O_7$ arose because the sample is not single phase. The stability of $BaTbO_3$ interferes with the formation of the superconducting material. However, when Tb is incorporated into the $RBa_2Cu_3O_7$ structure, it is trivalent, and it does not suppress superconductivity.

The mechanism involved in the suppression of superconductivity by Pr in $PrBa_2Cu_3O_7$ is complex and is a central focus of the issue of T_c suppression by f-ions in high-T_c oxides [3,18,19]. Initially it was argued that T_c suppression occurred through hole filling, and that Pr was mixed valent or tetravalent. This argument is supported by the chemistry of Pr, which is known to have stable trivalent and tetravalent states in oxidic systems. Initially magnetic susceptibility data were also used in support of mixed-valent Pr. Pr in $PrBa_2Cu_3O_7$ has a measured paramagnetic susceptibility that is intermediate between the free ion values of the trivalent and tetravalent ions.

Inelastic neutron scattering (INS) has been used extensively to characterize the electronic properties of the Pr f states in $PrBa_2Cu_3O_7$[7,20-25]. Whereas there are minor discrepancies about some of the peak assignments, the overall conclusions are clear. The data clearly show that Pr is trivalent in this compound. The linewidths of the magnetic peaks are unusually broadened in the spectra, indicating either static or dynamic processes are influencing the Pr electronic states. This effect is clearly demonstrated by a comparison of the INS data from $PrBa_2Cu_3O_7$ with those obtained form Pr_2CuO_4, shown in Figure 4. Despite the line broadening, it is clear that the INS data are consistent with a trivalent Pr ion that has a $^3H_4$ electronic ground level. This ground level is split by the orthorhombic symmetry into 9 singlets that are well represented by a crystal-field model similar to that

Figure 4. A comparison of the INS energy loss spectra obtained from (a) $PrBa_2Cu_3O_7$ and (b) Pr_2CuO_4. Both data sets were taken on the same spectrometer with the same experimental parameters. Solid line in (a) are data from $YBa_2Cu_3O_7$ to show the contribution from phonons over the same energy range. The * at zero energy transfer in (b) indicates elastic scattering.

found for other R in this compound[7,20]. The crystal-field splitting determined by fitting these data is somewhat unusual, in that there are two excited-state singlets within 4 meV of the ground state, with the next excited state located about 45 meV higher in energy. This splitting is depicted in Figure 5. The splitting of the ground level into a "pseudo-triplet" ground state, which is isolated from the higher states, results from the nearly cubic R-site symmetry. The magnitude and temperature dependence of the magnetic susceptibility can be entirely accounted for by this electronic structure of Pr^{3+}[20]. The calculated effective moment of $2.8\mu_B$ agrees well with that measured experimentally, and is significantly reduced from the free ion value of $3.58\mu_B$. There is no need to invoke mixed-valent behaviour to understand the susceptibility data. The reduced effective moment, together with the saturation moment of $0.79\mu_B$, measured in the ordered state[26,27], are understood in terms of a renormalization of the pseudo-triplet state[22].

Figure 5. A comparison of the splittings of thePr^{3+} $^3H_4$ ground term by the crystalline-electric field (CEF) generated at the R site in the $RBa_2Cu_3O_7$ (123), R_2CuO_4 (214), and $Pb_2Sr_2RCu_3O_8$ (PSYCO) structures [7]. Solid lines represent singlet states, dotted lines represent triplet states.

The majority of data suggest that Pr is trivalent in $PrBa_2Cu_3O_7$[7,19], thereby arguing against a charge-transfer, hole-filling mechanism for the suppression of T_c. The strongest supporting evidence in favour of a charge transfer model to explain suppressed a T_c in $PrBa_2Cu_3O_7$ comes from studies involving Ca substitution. A study of the superconducting behaviour of the solid-solution series $Y_{1-x-y}Ca_yPr_xBa_2Cu_3O_7$ shows that the substitution of Ca^{2+} for Pr restores superconductivity[28]. The argument presented is that Pr^{4+} removes holes from the CuO planes, which are subsequently restored by the addition of Ca^{2+}. Even more convincing is the report of superconductivity in the thin film $Pr_{.5}Ca_{.5}Ba_2Cu_3O_7$ at 43 K[29]. As we will point out our discussion of results from $Pb_2Sr_2Pr_{.5}Ca_{.5}Cu_3O_8$, there is an alternate explanation to hole filling that is consistent with the presence of Pr^{3+}[30].

The only other isostructural member of the $RBa_2Cu_3O_7$ series that can be made single phase but is not superconducting is the R=Cm analog[31]. X-ray diffraction data on $CmBa_2Cu_3O_7$ can be indexed on the Pmmm orthorhombic structure seen for the Y analog. The lattice constants are the same, within experimental error, as those obtained from $PrBa_2Cu_3O_7$. The inverse susceptibility is plotted as a function of temperature in Figure 6. There is no evidence of superconductivity over the temperature range studied, that is down to 10 K. The effective moment, determined from the slope of the inverse susceptibility, is (8.9 $\pm$ 0.4) μ_B. This high moment implies the full Cm^{3+} valence because Cm^{4+} has no magnetic moment, assuming Russell Sanders coupling (L=3; S=3; J=L-S=0)[32]. An expanded view of the low temperature behaviour is shown as an inset in Figure 6. The inflection in this data has a very similar appearance to that observed for the Pr analog [26] where neutron diffraction was used to show that the Pr moments order. Thus, the shape of the curve, together with the linearity of the M vs. H curve at 12 K in fields up to 5 T, suggests antiferromagnetic ordering of the Cm moments at 22 K.

Figure 6. The inverse magnetic susceptibitiy of $CmBa_2Cu_3O_7$ plotted versus temperature (a Curie plot). There is no evidence of superconductivity down to 4 K. An expanded view of the susceptibitiy in the low temperature range 10-50 K is shown in the inset. We interpret the cusp at 22 K as an indication of long-range magnetic ordering of the Cm moments.

Although $CmBa_2Cu_3O_7$ forms a single-phase member of the $RBa_2Cu_3O_7$ series, it does not superconduct. It is clear that Cm is trivalent in this compound, ruling out a charge transfer model. In addition, the Cm magnetic moments order at an unusually high temperature compared to the other isostructural $RBa_2Cu_3O_7$ compounds, except the R=Pr analog.

R_2CuO_4

The R_2CuO_4 series of compounds is isostructural for R=Pr-Gd and Cm. They crystallize with the K_2NiF_4-related T'-structure[33,34], which provides a significantly different crystal-field environment at the R site than found in the $RBa_2Cu_3O_7$ or the $Pb_2Sr_2RCu_3O_8$ series[7]. In addition, the magnetic transitions between states within the

ground multiplet are markedly different for Pr in Pr_2CuO_4 compared with Pr in $PrBa_2Cu_3O_7$, as observed by inelastic neutron scattering, As shown in Figures 4, the transitions for the former compound are narrow, resolution limited, whereas those seen for the latter compound are very broadened. The sample qualities, as judged by x-ray and neutron diffraction, are comparable. The line broadening seen for the $PrBa_2Cu_3O_7$ is attributed to a dynamic, lifetime effects, perhaps resulting from interactions with the Cu spins [7]. In addition to differences in linewidth, the magnetic transitions in these two materials occur at much different energies, as seen by the comparison of the splitting of the Pr^{3+} ground term in the R-site environments provided by the different structures. Pr^{3+} in the R_2CuO_4 compound has an isolated-singlet ground state, in contrast to the $RBa_2Cu_3O_7$ and $Pb_2Sr_2RCu_3O_8$ materials, in which Pr has an isolated pseudo-triplet ground state. This difference in ground state electronic properties manifests itself in the magnetic behaviour of Pr in these three structure types. Pr_2CuO_4 has only a very small moment at low temperature, $0.08\mu_B$ observed by neutron diffraction [35]. This moment is induced by the ordering on the Cu sublattice. There is no evidence of long range ordering of the Pr sublattice, in contrast to the other two series, in which the Pr analog orders at an anomalously high temperature with respect to other R in the same series. The Nd moments in R_2CuO_4 order at about T_N=1.3 K[35], T_N=5.95 K for the R=Sm[36], T_N=6.5 K for the R=Gd[37] and T_N=25 K for the R=Cm[38,39] analogs.

Superconductivity is achieved by replacing R^{3+} by Ce^{4+} (or Th^{4+}) to form $R_{1.85}Ce_{.15}CuO_4$[34], such that the superconducting carriers are electrons. The R ions Pr-Sm all form single-phase superconductors with T_c's of about 24 K. The solubility limit of Ce in the Gd analog is less than that required to induce superconductivity, which accounts for the absence of a transition in this material. The Pr analog has superconducting properties indistinguishable from other members of the series. In contrast, the Cm analog $Cm_{1.83}Th_{.17}CuO_4$ does not superconduct, although it is isostructural with the other T' compounds[38,39]. Instead, the antiferromagnetic ordering of the Cm moments is depressed from 25 K in the parent compound to 13 K for the Th-doped material, as shown in Figure 7. The effective moment obtained for Cm in both the parent and the doped compound is $(7.89\pm0.5)\mu_B$, which compares well with the free ion moment of Cm^{3+}.

In summary, $R_{1.83}Ce_{.17}CuO_4$ superconducts when R=Pr, but not when R=Cm. Both Pr and Cm are trivalent in this series. Pr has no local magnetic moment, whereas Cm as the full $7.89\mu_B$ associated with the trivalent s-state ion. These Cm moments order at anomalously high temperatures.

$Pb_2Sr_2RCu_3O_8$

The Pb-based series of compounds, $Pb_2Sr_2RCu_3O_8$, form for R=Y,La-Lu, Am, and Cm. This series is of considerable interest because the Ce, Pr and Tb analog all form, and therefore provide an ideal opportunity to study the effects of selected f-ions on superconducting properties. These compounds are essentially isostructural [40], with only slight distortions from the basic orthorhombic structure[41,42]. The R environment in $Pb_2Sr_2RCu_3O_8$ is very similar to that found in the $RBa_2Cu_3O_7$ series[43]. These materials are made superconducting by replacing 50% of the R^{3+} by Ca^{2+}. The excess holes are transferred to the CuO planes thought to be responsible for superconductivity. Superconductivity in these materials are reported as high as 84 K in single crystal samples,

Figure 7. (a) A Curie plot of the magnetic susceptibilty data obtained from Cm_2CuO_4. The effective moment obtained from these data is consistent with that expected for the Cm^{3+} free ion. (b) An expanded view of the low temperature susceptiblity. The cusp at 25 K is indicative of antiferromagnetic ordering of the Cm moments. This ordering has been confirmed by neutron diffraction. (c) The low temperature magnetic susceptibility of $Cm_{1.87}Th_{.13}CuO_4$. There is no evidence of superconductivity in this sample. The cusp in the susceptibility has moved down to 13 K from 25 K in the parent compound with the introduction of 8.5 % diamagnetic Th^{4+}.

with somewhat lower temperatures reported for powder samples synthesized by solid-state techniques. All the samples, including the R=Pr and Tb analogs can be made superconducting except for the R=Ce and Am analogs, which do not superconduct down to the lowest temperatures measured (4 K)[41,44]. The magnetic responses, as a function of temperature, for the R=Ce, Pr, Tb, and Am analogs are shown in Figure 8. The Tb analog has a T_c(onset)=71 K, which is typical of other R analogs including R=Gd, Ho, and Er samples that have been made by the same synthetic route. Whereas the R=Pr analog is also superconducting, its T_c is depressed by 10 K relative to the other superconductors in this series.

Figure 8. The low-field magnetization versus temperature data obtained from polycrystalline compounds of $Pb_2Sr_2R_{.5}Ca_{.5}Cu3O_8$ for R= Ce, Am, Pr, and Tb. These data show superconducting transitions for the R=Pr and Tb samples. There is no evidence of superconductivity in the R=Ce and Am samples.

The Am and Ce compounds do not superconduct down to 5 K, the lowest temperature measured. The structural and electronic behaviours of both of these compounds have been studied in detail [41,44] A comparative list of the lattice constants and R-O bond distances is provided in Table III. Both the Ce and Am analogs have R-O distances that are shorter than expected by comparison of other ions with similar trivalent ionic radii, suggesting that these ions may be tetravalent in this host. This suggestion is confirmed by an analysis of the XANES data shown in Figure 9. These edge spectra clearly show that Ce and Am are tetravalent. Magnetic susceptibility data obtained from $Pb_2Sr_2AmCu_3O_8$ support this conclusion. Neither of these samples show any indication of magnetic ordering down to the lowest temperature measured.

The absence of superconductivity in $Pb_2Sr_2Ce_{.5}Ca_{.5}Cu_3O_8$ and $Pb_2Sr_2Am_{.5}Ca_{.5}Cu_3O_8$ can then be understood in terms of charge transfer from Ce or Am to the CuO lattice. The reduced charge on the CuO planes, confirmed by Cu K edge XANES[41] (not shown), can account for the absence of superconductivity. Ca^{2+} substitution, which increases charge on the CuO sublattice, cannot be accomplished to high enough concentrations to sufficiently increase the charge on the CuO planes. It is argued that the

Table III. Lattice parameters (a, b, and c), cell volumes, and R-O near neighbour distances in $Pb_2Sr_2RCu_3O_8$. Structural data (except for R=Am) were obtained from refinement of powder neutron diffraction data based on the space group Cmmm[41]. The lattice parameters for the R=Am data were obtained from analysis of powder x-ray data, and the R-O bond distance was obtained from fitting EXAFS spectra[44].

R	a(Å)	b(Å)	c(Å)	Volume (Å^3)	R-O(Å)
Y	5.3943(1)	5.4337(1)	15.7251(2)	460.93(1)	2.3989(1)
Ce	5.4312(1)	5.4741(2)	15.8238(4)	470.45(2)	2.4857(2)
Pr	5.4449(1)	5.4836(1)	15.7982(3)	471.70(1)	2.4909(1)
Tb	5.4033(1)	5.4433(1)	15.7325(3)	462.72(1)	2.4213(1)
Am	5.411(3)	5.459(4)	15.822(8)	467.4(5)	2.22(7)

Figure 9. (a) A comparison of the Ce L_3-edge XANES from a trivalent standard (CeF_3) and a tetravalent standard (CeO_2) with data from$Pb_2Sr_2Ce_{1-x}Ca_xCu3O_8$ for x=0 and 0.5. The similarity of the edge features of the CeO_2 and the two Pb-based samples reveals that Ce is tetravalent in the latter compounds.

concentration of holes on the CuO planes is not sufficient to permit superconductivity. T_c in these two compounds is suppressed by a simple charge-transfer mechanism.

As seen from Figure 8, $Pb_2Sr_2Tb_{.5}Ca_{.5}Cu_3O_8$ is superconducting below 71 K. L_3-edge XANES measurements, shown in Figure 10, demonstrate that Tb is trivalent. Inelastic neutron scattering data support this conclusion. Crystal-field modeling of the data, using the crystal field scheme derived from work on the R=Ho and Er analogs[43,45], has been used to determine the splitting of the Tb^{3+} $^7F_6$ ground multiplet[46]. The wavefunctions, energies and symmetries of the crystal-field states are used to calculate the magnetic properties of the Tb analog. The strong anisotropy in the magnetic response from a single crystal of $Pb_2Sr_2TbCu_3O_8$[46] is well reproduced by the calculations. However, the observed χ(parallel) deviates considerably for the calculation at temperatures below about 120 K, as does the powder data, shown in Figure 11. For comparison, the figure also includes data obtained from a 5%Tb in Y sample, $Pb_2Sr_2Tb_{.05}Y_{.95}Cu_3O_8$. It can be seen that the

susceptibility data obtained from the 5% Tb compound are very different from those obtained from the pure R=Tb sample, and that the data from the magnetically dilute sample agree very well with the calculated susceptibility. We interpret this behaviour to the effects of Tb-Tb spin interactions that persist to very high temperatures. These interactions are strongly suppressed in the diluted system. Support for this observation comes from the unusual temperature dependence of the INS elastic line [46]. Both the magnetic susceptibility and the INS data show deviations from expected single-ion behaviour at temperatures less than 120 K. Neutron diffraction experiments[47] on the parent compound reveal a quasi two dimensional (2D) phase with finite antiferromagnetic correlations along the c-direction together with a three dimensional phase with ferromagnetic correlations along the c-direction. The co-existence of the two phases is likely to be related to structural imperfections such as stacking faults, strains, oxygen disorder or cation vacancies. The $Pb_2Sr_2Tb_{.5}Ca_{.5}Cu_3O_8$ sample, which has a superconducting critical temperature of 71 K, also exhibits a quasi 2D magnetic ordering of the Tb sublattice with a finite ferromagnetic correlation along the c-direction. These magnetic correlations are more than an order of magnitude higher than seen in any related system, as well as much higher than the two-dimensional long-range ordering temperature of T_N=5.3 K [48] for the parent compound. This unusual behaviour is understood in terms of the highly two dimensional nature of the lattice combined with the strongly Ising-like magnetic properties.

Figure 10. Tb L_3-edge XANES from $Pb_2Sr_2TbCu_3O_8$ are compared with a trivalent standard ($TbCl_3$) as well as mixed trivalent and tetravalent (Tb_4O_7) and tetravalent ($SrTbO_3$) standards. The comparison demonstrates that Tb is trivalent in the Pb-based sample.

The Tb moments in $Pb_2Sr_2TbCu_3O_8$ order at a high temperature relative to the other members of the series, except the Pr analog. For example, the Gd moments order at T_N=2.3 K[49]. The relatively high Neel temperature found for the Tb moments in $Pb_2Sr_2TbCu_3O_8$ is understood in terms of the effects of a small molecular field on the quasi-doublet ground state[47]. A large longitudinal transition strength strongly enhances the susceptibility in the c-direction and suppresses the perpendicular susceptibility, relative to an isotopic ion such as

Gd, in a similar environment. There appears to be no need in the Tb case for any additional exchange interactions or hybridization to explain its unusually high T_N in these double-layer cuprates.

The Pr analogs of the $Pb_2Sr_2R_{1-x}Ca_xCu_3O_8$ series provide unique information on the role of Pr in suppressing high T_c superconductivity. $Pb_2Sr_2PrCu_3O_8$ is isostructural with the other members of this series. Pr in this compound sits in a site structurally very similar to that of Pr in $PrBa_2Cu_3O_7$. The parent compound exhibits semiconducting behaviour and has a magnetically ordered Pr sublattice below $T_N \approx 5.8K$[50,51], which is a higher T_N than that observed for $Pb_2Sr_2GdCu_3O_8$, but lower than the T_N=17K observed for $PrBa_2Cu_3O_7$[26]. The magnetic ordering temperatures of the Gd analogs of these two compounds are comparable. The magnetic structure at low temperature, determined from neutron diffraction experiments[52]. is similar to that observed for the Tb analog The saturation moment of $1.4\pm0.4\mu_B$ for Pr is slightly larger than the $0.79\pm.04\mu_B$ found in $PrBa_2Cu_3O_7$.

Figure 11. A comparison of the susceptibilities measured from powdered samples of $Pb_2Sr_2TbCu_3O_8$ (open circles) and the magnetically dilute sampe $Pb_2Sr_2Tb_{.05}Y_{.95}Cu_3O_8$ (full circles). These data are compared with single-ion CEF calculations (solid line).

The INS data from $Pb_2Sr_2PrCu_3O_8$ reveal the expected similarities for the electronic properties of Pr in this and the $PrBa_2Cu_3O_7$ structure[52]. The magnetic-scattering lines are significantly broadened over that expected from the experimental resolution, as is demonstrated in Figure 4 for $PrBa_2Cu_3O_7$. Overall, the splitting of the Pr^{3+} $^3H_4$ ground level is similar in both materials, including the splitting of the lowest three singlets. The splittings of the Pr^{3+} ground levels for the various compounds of interest herein are depicted schematically in Figure 5. There overall splitting is about 4 meV in both materials, and they are well isolated from higher energy states, resulting in a quasi-triplet ground state, that renormalizes at low temperatures to result in a local, ordered moment on Pr [22,52].

In order to induce superconductivity, it is necessary to replace approximately 20-80% of the Pr^{3+} in $Pb_2Sr_2PrCu_3O_8$ with Ca^{2+}. The holes introduced by this substitution reside in the CuO planes, and are the superconducting carriers. $Pb_2Sr_2Pr_{.5}Ca_{.5}Cu_3O_8$ is a

superconductor similar to the other R members of this series, except that T_c is about 60K, reduced by 10K from the other members of the series. The long-range ordering of the Pr moments is suppressed by this substitution.

In addition to the effect that the Ca^{2+} substitution has on the electronic properties of the CuO sublattice, it also has an effect on the single-ion electronic properties of the R ions. This has been explicitly demonstrated for Ca substitution in $Pb_2Sr_2ErCu_3O_8$[45], where the Er states are shown to broaden and slightly shift in energy with Ca substitution. This change in the Er states is understood to result from a statistical distribution of Ca second near neighbours, which slightly modifies the CEF potential. A comparison of low energy INS data obtained from undoped and doped $Pb_2Sr_2PrCu_3O_8$, shown in Figure 12, reveals a similar effect in this case. The effect of Ca substitution on the Pr INS data is to broaden the magnetic peaks, and to shift the magnetic scattering of the quasi triplet to higher energies. This increased splitting of the quasi triplet with Ca substitution could be interpreted as effectively reducing the number of magnetic Pr ions, or as an increase of the average CEF splitting and therefore a reduction in the average magnetic moment on the Pr ions. This result is extremely important because it demonstrates that the role of Ca substitution is more complex than initially understood. Not only does Ca substitution alter the number of carriers in the CuO planes, it also alters the single ion magnetic properties of the R ions, which we argue can have a significant influence on the bulk properties exhibited by the material.

Preliminary data are available on $Pb_2Sr_2CmCu_3O_8$. X-ray powder diffraction data show this compound to form as a single phase material, with lattice constants very similar to those obtained from the Pr analog under similar conditions[53]. Susceptibility data as a function of temperature show a cusp at 15 K, which is attributed to antiferromagnetic ordering of the Cm sublattice. Neutron diffraction measurements are planned to confirm this finding.

Figure 12. A comparison of detail-balance corrected INS energy spectra obtained from $Pb_2Sr_2Pr_{1-x}Ca_xCu_3O_8$ for x=0 and 0.5. Data are normalized per mole Pr ions at 20 K. (a) Low energy transfer region shows sharply lower intensity for the x=0.5 sample. (b) Magnetic scattering of the x=0.5 sample is seen to extend out to higher energies. These data indicate that the ground state splitting of Pr in this materials is influenced by the incorporation of Ca. The energy splitting of the pseudo-triplet ground state, about 4 meV for the x=0 compound, is expanded to about 14 meV in the Ca-doped sample

DISCUSSION AND CONCLUSIONS

The results of this systematic study on the Ce, Pr, Tb, Am and Cm analogs of the three superconducting series $RBa_2Cu_3O_7$, $R_{2-x}M_xCuO_4$, and $Pb_2Sr_2R_{1-x}Ca_xCu_3O_8$ are summarized in Table IV. These results can be divided into 4 main categories: (1) compounds that do not form, i.e. $CeBa_2Cu_3O_7$ and $TbBa_2Cu_3O_7$; (2) compounds in which R is tetravalent, i.e. $Pb_2Sr_2Ce_{1-x}Ca_xCu_3O_8$ and $Pb_2Sr_2Am_{1-x}Ca_xCu_3O_8$. T_c is suppressed in these compounds; (3) compounds which form the correct phase, R is essentially trivalent, and T_c is suppressed, i.e. $PrBa_2Cu_3O_7$, $CmBa_2Cu_3O_7$, Cm_2CuO_4 and $Pb_2Sr_2CmCu_3O_8$; and (4) superconducting compounds, i.e. $Pr_{1.82}Ce_{.18}CuO_4$, $Pb_2Sr_2Pr_{.5}Ca_{.5}Cu_3O_8$, and $Pb_2Sr_2Tb_{.5}Ca_{.5}Cu_3O_8$. It is informative to compare and contrast these categories.

Table IV. A summary of the work presented herein. For full references, see text.

	$Y_{1-x}R_xBa_2Cu_3O_7$ $T_c \approx 92$ K	**$R_{1.85}M_{0.15}CuO_4$ $T_c \approx 20$ K**	**$Pb_2Sr_2R_{1-x}Ca_xCu_3O_8$ $T_c \approx 80$ K**
Ce	4+ ($x < 0.1$) suppresses T_c	Does not form	4+ suppresses T_c
Pr	3+ ($x \leq 1$) suppresses T_c $T_N = 17$ K	3+ normal T_c	3+ lower (T_c=60K) $T_N = 6$ K
Tb	3+ ($x = 0.3$) normal T_c	Does not form isostructural phase	3+ normal T_c $T_N = 5.3$ K
Am	$BaAmO_3 + Cu_2O$	$AmO_2 + Cu_2O$	4+ suppresses T_c
Cm	3+ ($x \leq 1$) suppresses T_c $T_N = 21$K	3+ suppresses T_c $T_N = 25$ K	3+ ($T_N = 15$ K)

There are several compounds in which T_c appears to be suppressed by the f-ion. For those compounds in which R is tetravalent, $Pb_2Sr_2Ce_{1-x}Ca_xCu_3O_8$ and $Pb_2Sr_2Am_{1-x}Ca_xCu_3O_8$, the mechanism for T_c suppression is expected to be one of simple charge transfer and resultant CuO hole filling. This proposed mechanism is supported by experimental results for $Pb_2Sr_2Ce_{1-x}Ca_xCu_3O_8$[41].

For the case in which R is trivalent but T_c is suppressed, the situation is much more complex, but several trends emerge. This category is restricted to samples that contain either Pr or Cm. These ions have similar ionic radii, similar 4+/3+ redox couples (see Table II), and they both have f-orbitals whose radial extent permits limited hybridization with neighbouring ligand states. Cm^{3+} ($5f^7$) is an s-state ion and therefore it has a large magnetic

moment that is unaffected to first order by crystal-field effects[32]. Cm suppresses superconductivity in all the compounds in which it is incorporated. In addition to suppressing superconductivity, the local moments on Cm also exhibit long-range ordering at temperatures an order of magnitude higher than superconducting members of the same series, as shown in Table IV.

Pr^{3+} also suppresses superconductivity. It has a $4f^2$ configuration with single-ion magnetic properties that depend significantly on the details of the crystal field magnitude and symmetry. For orthorhombic or lower site symmetry the $^3H_4$ ground level is split into 9 singlets. The details of this splitting play a central role in determining the single-ion and collective properties of samples containing Pr. The relative energies of the singlet states in $PrBa_2Cu_3O_x$ and $Pb_2Sr_2PrCu_3O_8$ are such that there is an effective ground-state triplet that is isolated from other, higher energy singlets. The result is that Pr^{3+} has an effective moment that is reduced from its free-ion value, and an ordered saturation moment at lower temperatures. Like Cm, the Pr analogs of these two compounds have Neel temperatures that are nearly an order of magnitude higher than those for the superconducting members of these series. In contrast to this behaviour, Pr_2CuO_4 has an isolated singlet ground state, no local moment at low temperature, and it is superconducting when appropriately doped. These results suggest that Pr suppresses superconductivity only when it has a local moment.

The influence of a Pr local moment on superconductivity is explored with the work on $Pb_2Sr_2Pr_{1-x}Ca_xCu_3O_8$. The data demonstrate that when x=0, the Pr ground multiplet is similar to that found in $PrBa_2Cu_3O_x$. The Pr-Pr magnetic interactions are sufficiently strong that magnetic ordering is induced at 6K in the undoped x=0 compound; an ordering temperature comparable to that found for $PrBa_2Cu_3O_6$ with $T_N \approx 10K$[54]. When Ca replaces some Pr in the Pb-based compound, the average splitting of the Pr^{3+} pseudo-triplet is increased, as evidenced by INS data shown in Figure 12. We argue that $Pb_2Sr_2Pr_{0.5}Ca_{0.5}Cu_3O_8$ superconducts, but T_c remains slightly suppressed because the pseudo-triplet splitting is not large enough to remove all moment from the ground state.

This analysis of the electronic and magnetic properties of Pr in the $RBa_2Cu_3O_7$, $R_{2-x}Ce_xCuO_4$, and $Pb_2Sr_2R_{1-x}Ca_xCu_3O_8$, taken together with the data on the Cm analogs of these materials provide a platform on which to build a fundamental understanding of the selective suppression of high-T_c superconductivity. The relevance of the magnetic ground state, specifically the size of the quasi-triplet ground-state splitting, to T_c suppression may affect the f-state hybridization with the CuO band states. It is possible that an increased quasi-triplet splitting may inhibit an effective hybridization between the 4f- and the CuO states. A non-magnetic singlet may not be able to hybridize effectively with the CuO states. Such effects are well known in Kondo systems, in which the CEF energy splitting can compete with the Kondo hybridization[55]. Of the f-ions that form superconducting or related phases, Pr and Cm have the most extended occupied f-orbitals, relative to the outer p- and d-orbitals, which allows them to most effectively hybridize with the CuO states. However, this alone is not sufficient to suppress superconductivity, as evidenced by the superconductivity observed for $Pr_{1.85}Ce_{.15}CuO_4$. In addition, there must be unpaired spins in the hybridizing states. We argue that it is the magnetic moments in hybridizing states that interact with the CuO states to suppress T_c. Whereas to date there is no direct information on the hybridization strength in these systems, this argument is strongly supported by the high

magnetic ordering temperatures observed for all Pr and Cm compounds that do not superconduct.

The theory of hole localization proposed by Fehrenbacher and Rice[4] can explain selected x-ray absorption and optical reflectivity data. However, the proposed admixture of 50% Pr^{+3} ($4f^2$) and Pr^{+4} ($4f^1$) is not consistent with the overall INS results. The magnetic data from Pr is well understood in terms of Pr^{3+} ions only. The Cm data are even more definitive in this regard ($\mu_{eff}(Cm^{3+}) = 7.94\mu_B$; $\mu_{eff}(Cm^{4+}) = 0\mu_B$). Certainly it has not been demonstrated how a mixing of Pr^{3+} and Pr^{4+} can explain the high ordering temperatures of the Pr and Cm moments. In contrast, the theory developed by Guo and Temmerman[6] is consistent with the results discussed herein.

Of the 4 mechanisms often proposed to explain the suppression of superconducting in $PrBa_2Cu_3O_7$, it is clear that simple charge transfer is not sufficient Although a full understanding of the fundamental mechanism for the suppression of T_c in these systems is yet to be attained, the current results clearly point toward the central role played by magnetic interactions. Further progress on this problem may necessitate an understanding of interactions responsible for high temperature superconductivity.

ACKNOWLEDGMENTS

The authors wish to thank C.W. Williams, S. Skanthakumar, G.L. Goodman, M.R. Antonio and C.-K. Loong for their contributions to aspects of this project. This work is supported by the U.S. DOE - Basic Energy Sciences, Chemical Sciences, under contract W31-109-ENG-38.

REFERENCES

[1]L. F. Schneemeyer, J. V. Waszczak, S. M. Zahurak, R. B. van Dover, and T. Siegrist, Mater. Res. Bull. **22**, 1467 (1987).

[2]S.E. Brown, J.D. Thompson, J.O. Willis, R.M. Aikin, E. Zirngiebl, J.L. Smith, Z. Fisk, and R.B. Schwarz, Phys. Rev. B **36**, 2298 (1987).

[3]L. Soderholm, K. Zhang, D. G. Hinks, M. A. Beno, J. D. Jorgenson, C. U. Segre, and I. K. Schuller, Nature **328**, 604 (1987).

[4]R. Fehrenbacher and T. M. Rice, Phys. Rev. Lett. **70**, 3471 (1993).

[5]A. I. Liechtenstein and I. I. Mazin, Phys. Rev. Lett. **74**, 1000 (1995).

[6]G. Y. Guo and W. M. Temmermann, Phys. Rev. B **41**, 6372 (1990).

[7]U. Staub and L. Soderholm, *Handbook on the Physics and Chemistry of Rare Earths* (in the press).

[8]M.B. Maple, L.E. DeLong, and B.C. Sales, "Kondo Effect: alloys and compounds," in *Handbook on the Physics and Chemistry of the Rare Earths*, edited by Karl A. Gschneidner and LeRoy Eyring (Elsevier, Amsterdam, 1978), Vol. 1, pp. 797.

[9]Peter Fulde, *Electron Correlations in Molecules and Solids*, 3rd ed. (Springer, Berlin, 1995).

[10]L R Morss, "Comparative Thermochemical and Oxidation-Reduction Properties of Lanthanides and Actinides," in *Handbood on the Physics and Chemistry of Rare Earths*, edited by K A Gschneidner, Jr., L Eyring, G R Choppin, and G H Lander (Elsevier Science, Amsterdam, 1994), Vol. 18, pp. 239.

[11]R.D. Shannon, Acta Crystallogr. A **32**, 751 (1976).

[12]Darleane Hoffman, private communication.

[13]Barry T. Kilbourn, *A Lanthanide Lanthology* (Molycorp, Inc., White Plains, 1993).

[14]C. R. Fincher, Jr., and Graciela B. Blanchet, Phys. Rev. Lett. **67**, 2902 (1991).

[15]U. Staub, L. Soderholm, S. Skanthakumar, and M.R. Antonio, J. Phys. IV France 7 **C2**, 1077 (1997).

[16]K. I. Gnanasekar, A. S. Tamhane, R. Pinto, R. Nagarajan, M. Sharon, L. G. Gupta, and R. Vijayaraghavan, Physica C **219**, 183 (1994).

[17]U. Staub, Mark R. Antonio, L. Soderholm, M. Guillaume, W. Henggeler, and A. Furrer, Phys. Rev. B **50**, 7085 (1994).

[18]Y. Dalichaouch, M. S. Torikachvili, E. A. Early, B. W. Lee, C. L. Seaman, K. N. Yang, H. Zhou, and M. B. Maple, Solid State Comm. **65**, 1001 (1988).

[19]H.B. Radousky, J. Mater. Res. **7**, 1917 (1992).

[20]L. Soderholm, C.-K. Loong, G. L. Goodman, and B. D. Dabrowski, Phys. Rev. B **43**, 7923 (1991).

[21]S. Skanthakumar, W-H. Li, J. W. Lynn, A. Kebede, J. E. Crow, and T. Mihalsin, Physica B **163**, 239 (1990).

[22]G.L. Goodman, C.-K. Loong, and L. Soderholm, J. Phys.: Condens. Matter **3**, 49 (1991).

[23]H.-D. Jostarndt, U. Walter, J. Harnischmacher, J. Kalenborn, A. Severing, and E. Holland-Moritz, Phys. Rev. B **46**, 14872 (1992).

[24]V. Nekvasil, E. Holland-Moritz, H.-D. Jostarndt, U. Walter, and G. Hilscher, J. Magn. Magn. Mater. **117**, 11 (1992).

[25]G. Hilscher, E. Holland-Moritz, T. Holubar, H.-D. Jostarndt, V. Nekvasil, G. Schaudy, U. Walter, and G. Fillion, Phys. Rev. B **49**, 535 (1994).

[26]W.-H. Li, J. W. Lynn, S. Skanthakumar, and T. W. Clinton, Phys. Rev. B **40**, 5300 (1989).

[27]S. Skanthakumar, J.W. Lynn, N. Rosov, G. Cao, and J.E. Crow, Phys. Rev. B **55**, R3406 (1997).

[28]J.J. Neumeier, T. Bjornholm, M.B. Maple, and Ivan K. Schuller, Phys.Rev. Lett. **63**, 2516 (1989).

[29]David P. Norton, D.H. Lowndes, B.C. Sales, J.D. Budai, B.C. Chanourmakos, and H.R. Kerchner, Phys.Rev.Lett. **66**, 1537 (1991).

[30]U. Staub, L. Soderholm, S. Skanthakumar, R. Osborn, and F. Fauth, Europhys. Lett. **39**, 663 (1997).

[31]L. Soderholm, G.L. Goodman, U. Welp, C.W. Williams, and J. Bolender, Physica C **161**, 252 (1989).

[32]G.K. Liu, J.V. Beitz, and Jin Huang, J. Chem. Phys. **99**, 3304 (1993).

[33]R. Saez Puche, M. Norton, T.R. White, and W.S. Glaunsinger, J. Solid State Chem. **50**, 281 (1983).

[34]H. Takagi, S.Uchida, and Y. Tokura, Phys.Rev.Lett **62**, 1197 (1989).

[35]M. Matsuda, K. Yamada, K. Kakurai, H. Kadowaki, T.R. Thurston, Y. Endoh, Y. Hidaka, R.J. Birgeneau, M.A. Kastner, P.M. Gehring, A.H. Moudden, and G. Shirane, Phys.Rev.B **42**, 10098 (1990).

[36]I.W. Sumarlin, S. Skanthakumar, J.W. Lynn, J.L. Peng, Z.Y. Li, W. Jiang, and R.L. Greene, Phys.Rev.Lett. **68**, 2228 (1992).

[37]J.D. Thompson, S.-W. Cheong, S.E. Brown, Z. Fisk, S.B. Oseroff, M. Tovar, D.C. Vier, and S. Schultz, Phys.Rev. B **39**, 6660 (1989).

[38]L. Soderholm, C.W. Williams, and U. Welp, Physica C **179**, 440 (1991).

[39]L. Soderholm, C.W. Williams, and S. Skanthakumar, (to be published).

[40]S. Skanthakumar and L. Soderholm, unpublished .

[41]S. Skanthakumar and L. Soderholm, Phys. Rev. B **53**, 920 (1996).

[42]U. Staub, L. Soderholm, S. Skanthakumar, P. Pattison, and K. Conder, Phys.Rev.B **57**, 5535 (1998).

[43]L. Soderholm, C.-K. Loong, J. S. Xue, J.P. Hammonds, J.E. Greedan, and M. Maric, J. Appl. Phys. **73**, 6314 (1993).

[44]L. Soderholm, Clayton Williams, S. Skanthakumar, Mark R. Antonio, and S. Conradson, Z. Phys. B **101**, 539 (1996).

[45]L. Soderholm, C.-K. Loong, U. Staub, S. Skanthakumar, J. S. Xue, J. P. Hammonds, J. E. Greedan, and M. Maric, Physica C **246**, 11 (1995).

[46]U. Staub, L. Soderholm, S. Skanthakumar, and Mark. R. Antonio, Phys. Rev. B **52**, 9736 (1995).

[47]U. Staub, L. Soderholm, S. Skanthakumar, S. Rosenkranz, C. Ritter, and W. Kagunya, Z. Phys. B. **104**, 37 (1997).

[48]C. R. Shih, T. H. Meen, Y. C. Chen, and H. D. Yang, Phs. Rev. B **50**, 9619 (1994).

[49]C.C. Lai, J.H. Shieh, B.S. Chiou, J.C. Ho, and H.C. Ku, Phys. Rev. B **49**, 1499 (1994).

[50]W. T. Hsieh, W-H. Li, K. C. Lee, J. W. Lynn, J. H. Shieh, and H. C. Ku, J. Appl. Phys **76**, 7124 (1994).

[51]J. H. Shieh, H. C. Ku, and J. C. Ho, Phys. Rev. B **50**, 3288 (1994).

[52]U. Staub, L. Soderholm, S. Skanthakumar, R. Osborn, F. Fauth, and C. Ritter, (to be published).

[53]L. Soderholm, C.W. Williams, and S. Skanthakumar, (unpublished).

[54]A. Kebede, J.P. Rodrigquez, I. Perez, T. Mihalsisin, G. Myer, J.E. Crow, P.P. Wise, and P.Schlottmann, J. Appl. Phys. **69**, 5376 (1991).

[55]S. Watanabe and Y. Kuramoto, Z. Phys. B **104**, 535 (1997).

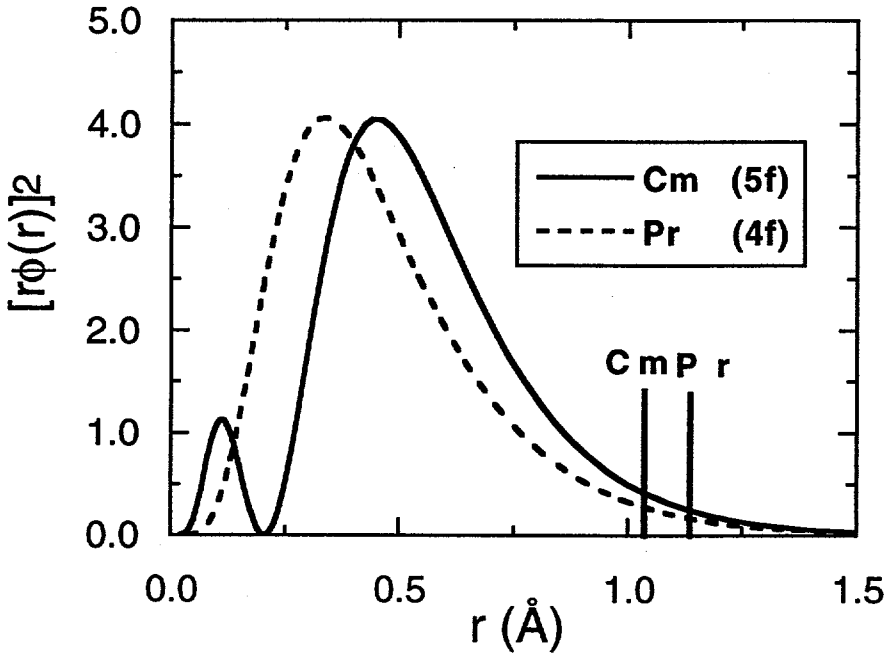

Sodérholm + Staub

Figure 1

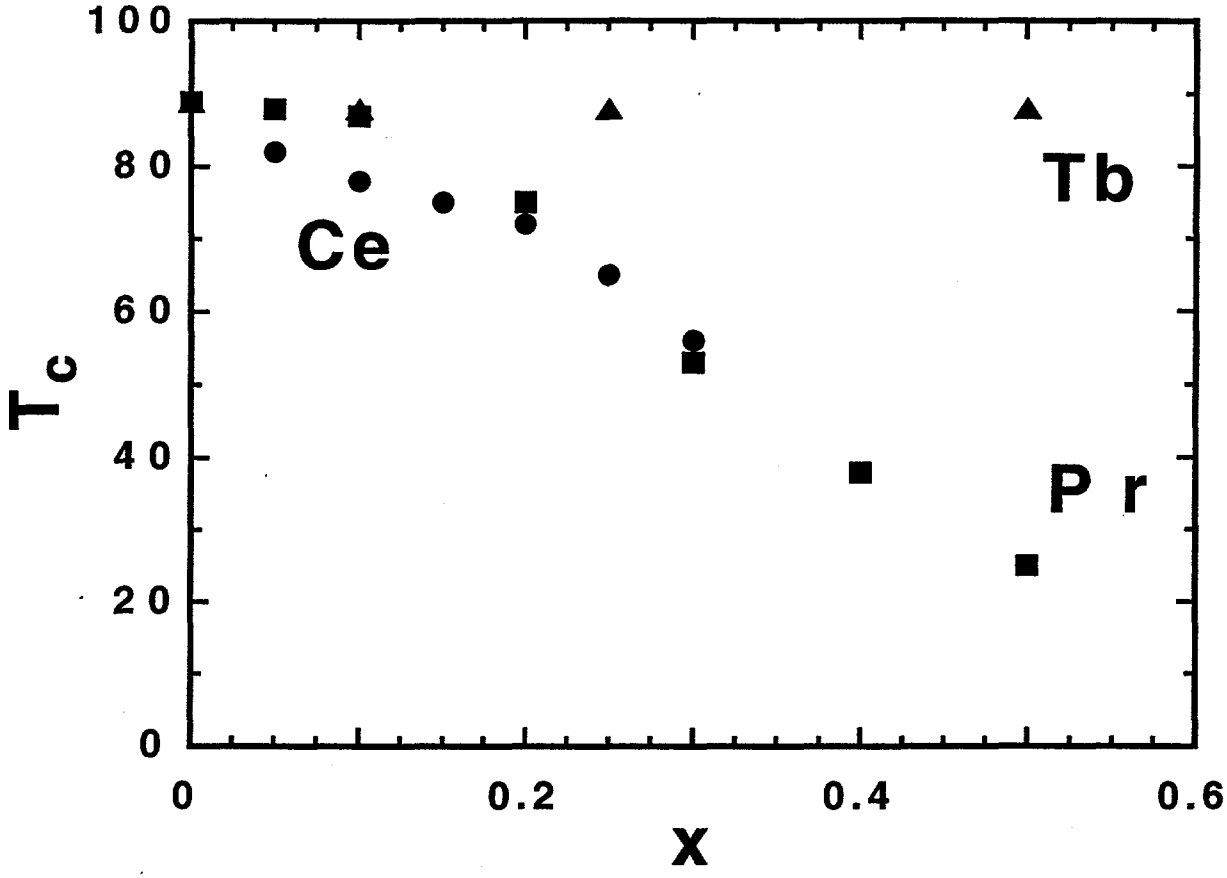

Soderholm + Staub

Figure 2

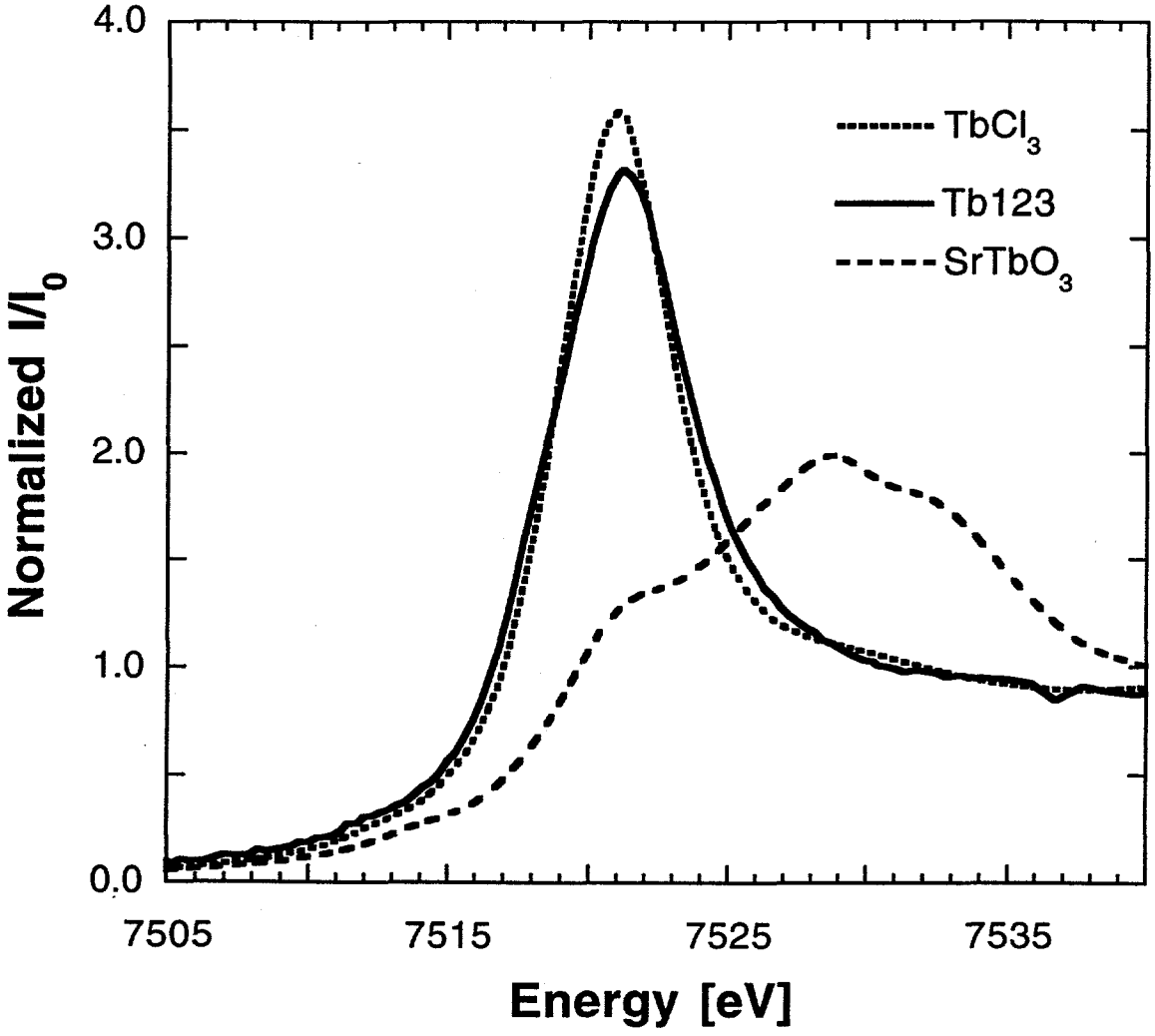

Soderholm + Staub
Figure 3

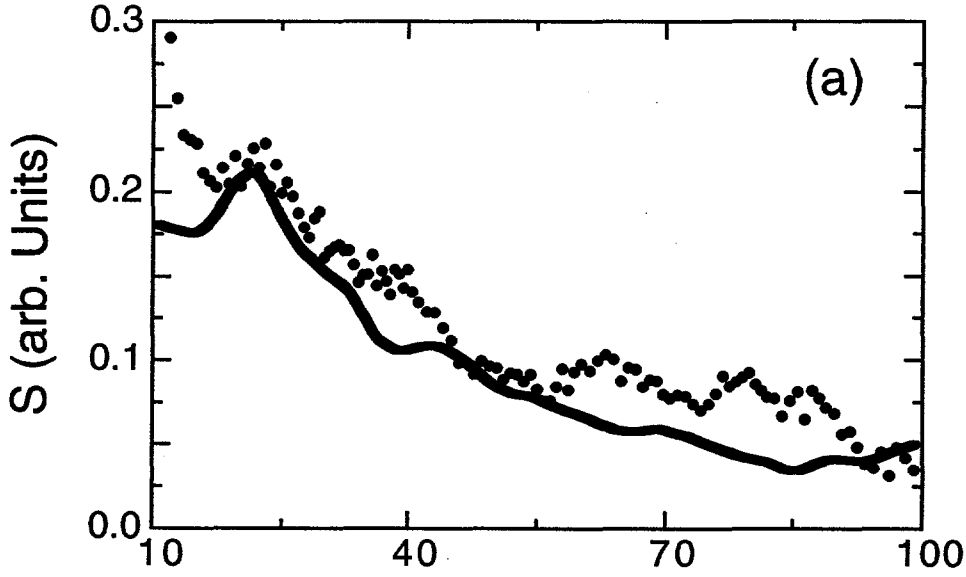

Soderholm and Staub

Figure 4a

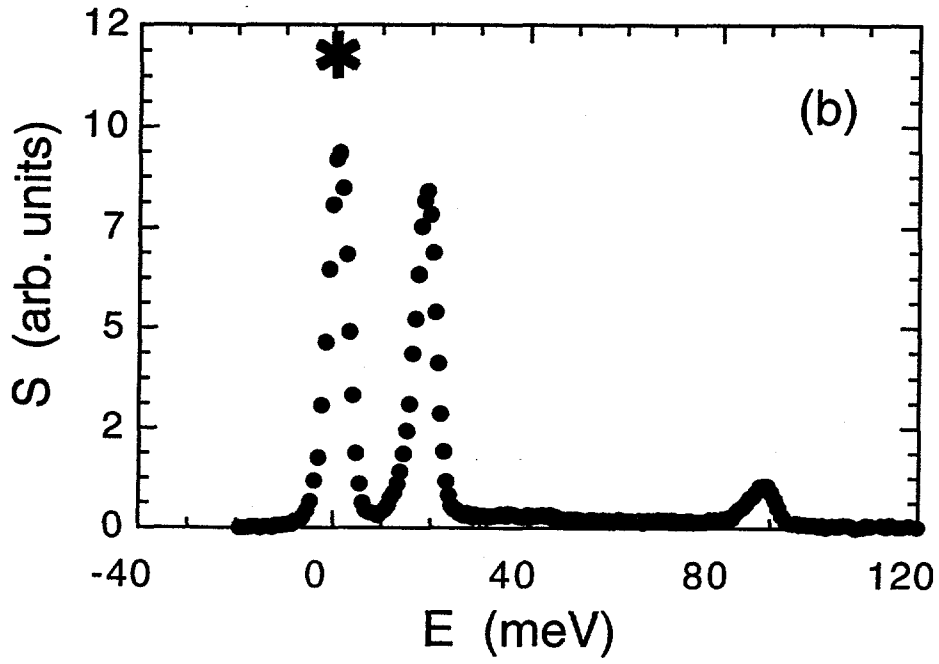

Soderholm and Staub

Figure 4b

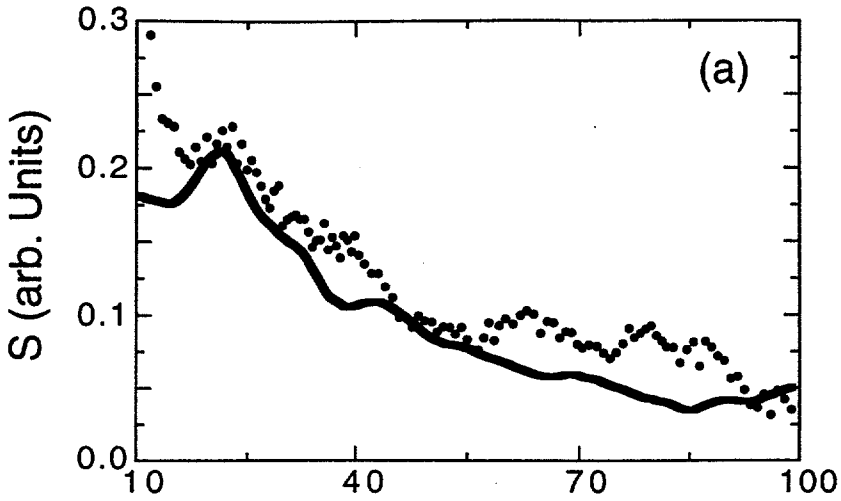

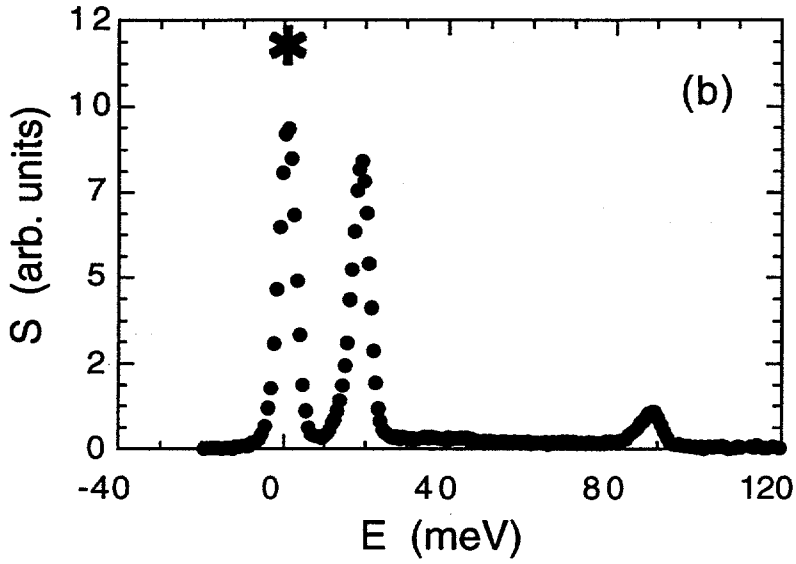

Soderholm and Staub
Figures 4a + b layout

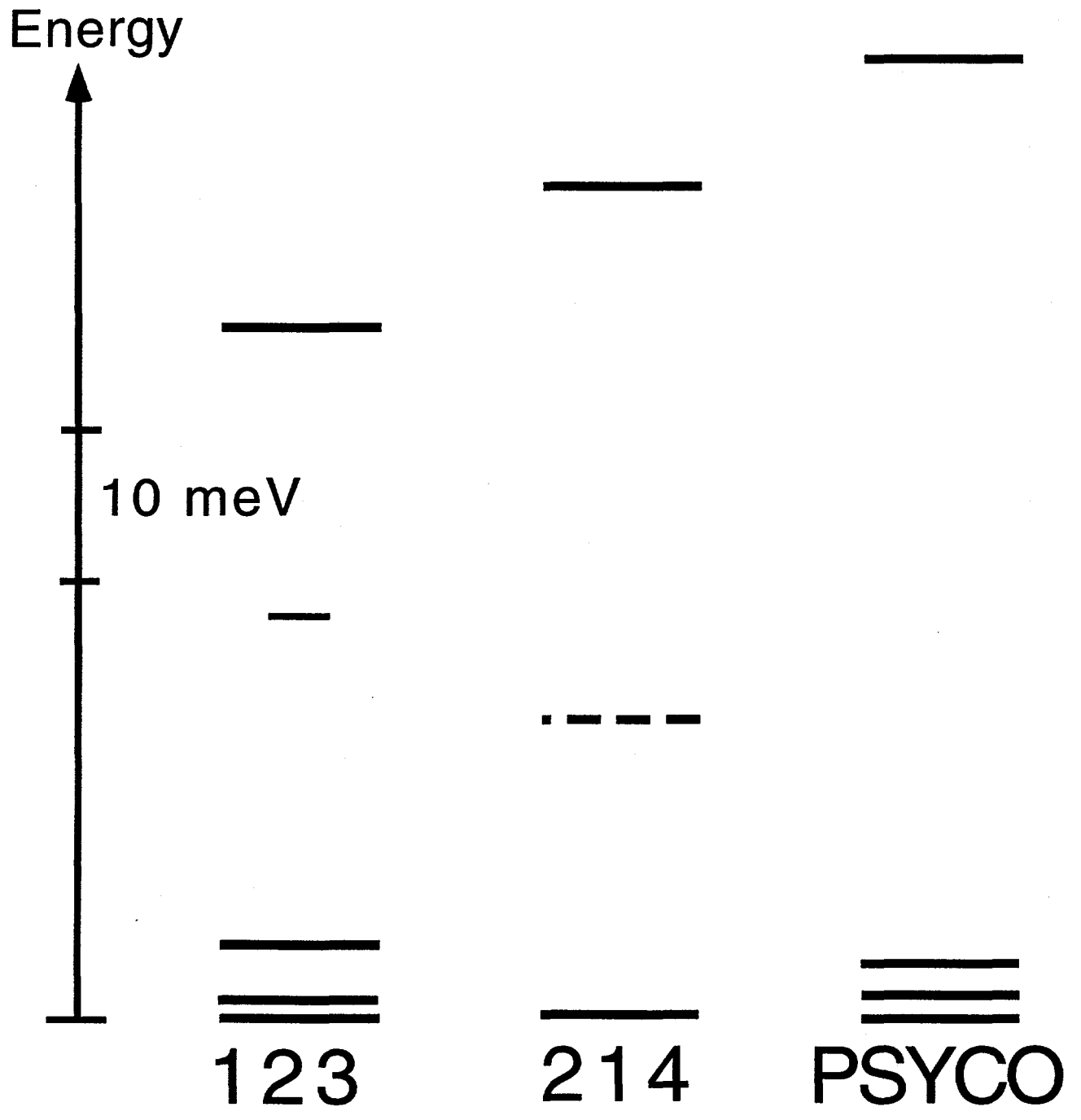

Soderholm and Staub

Figure 5

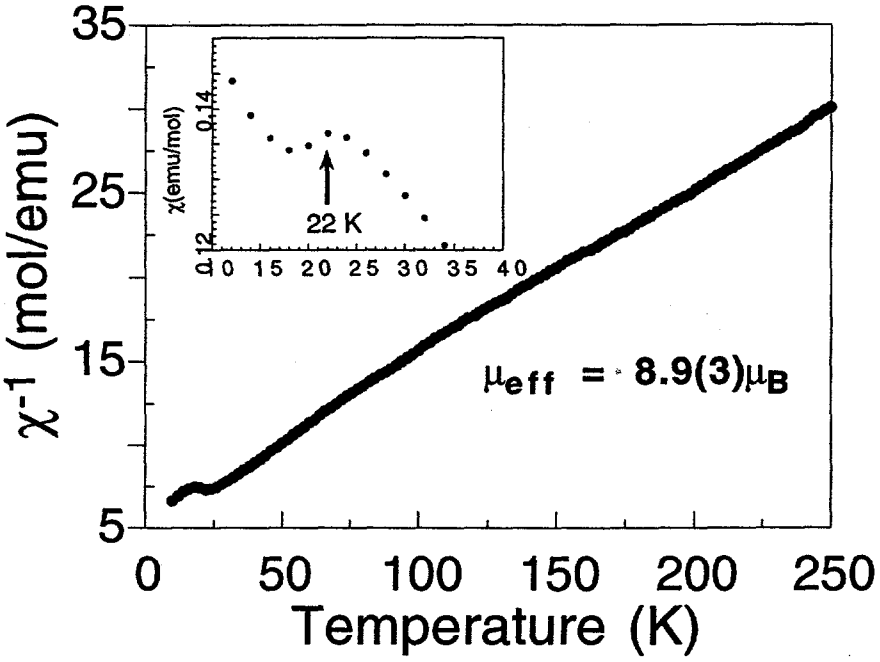

Soderholm and Staub
Figure 6

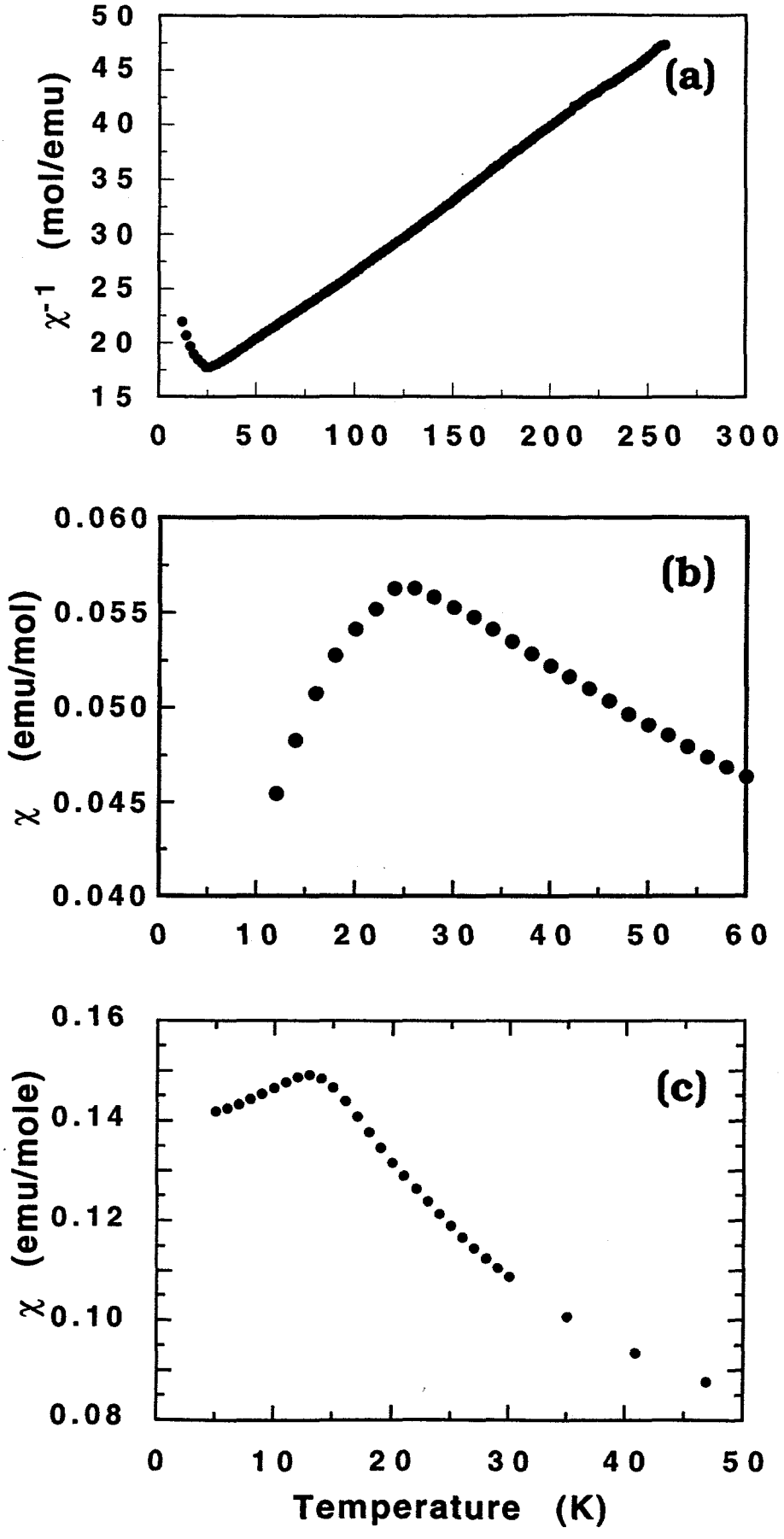

Soderholm and Staub Figure 7

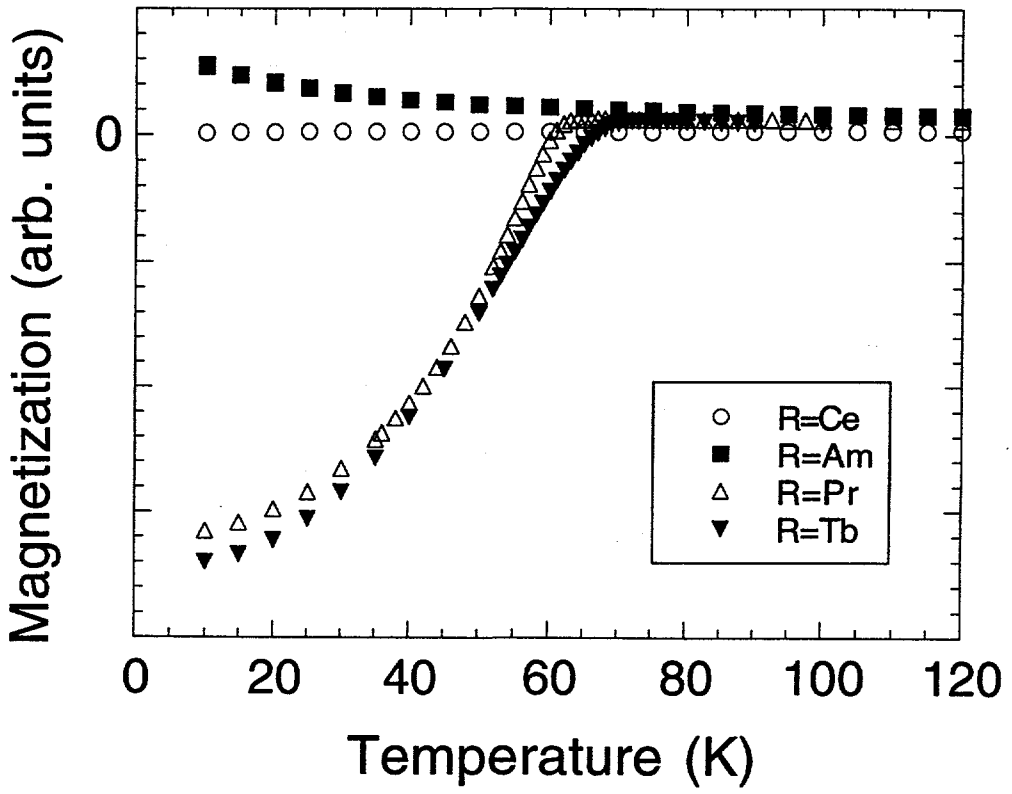

Soderholm and Staub
Figure 8

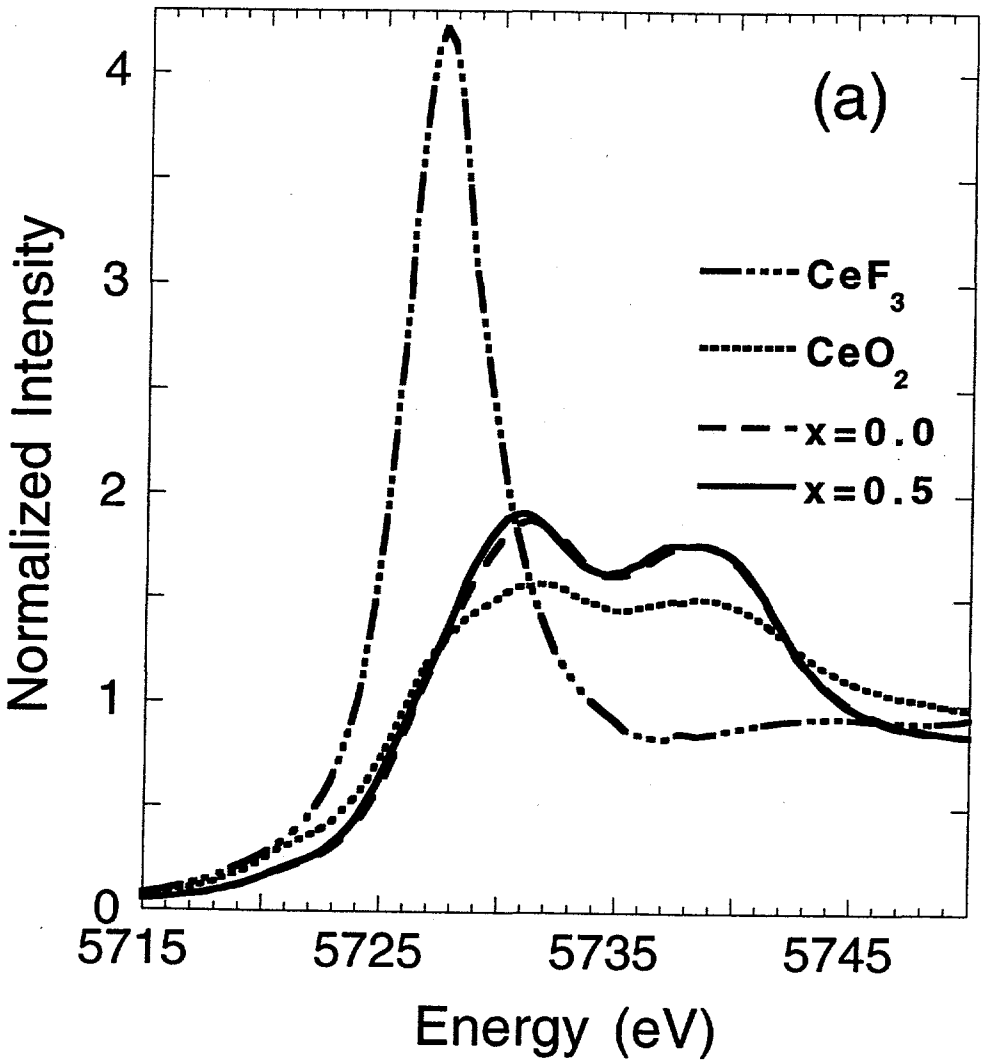

Soderholm and Staub
Figure 9a

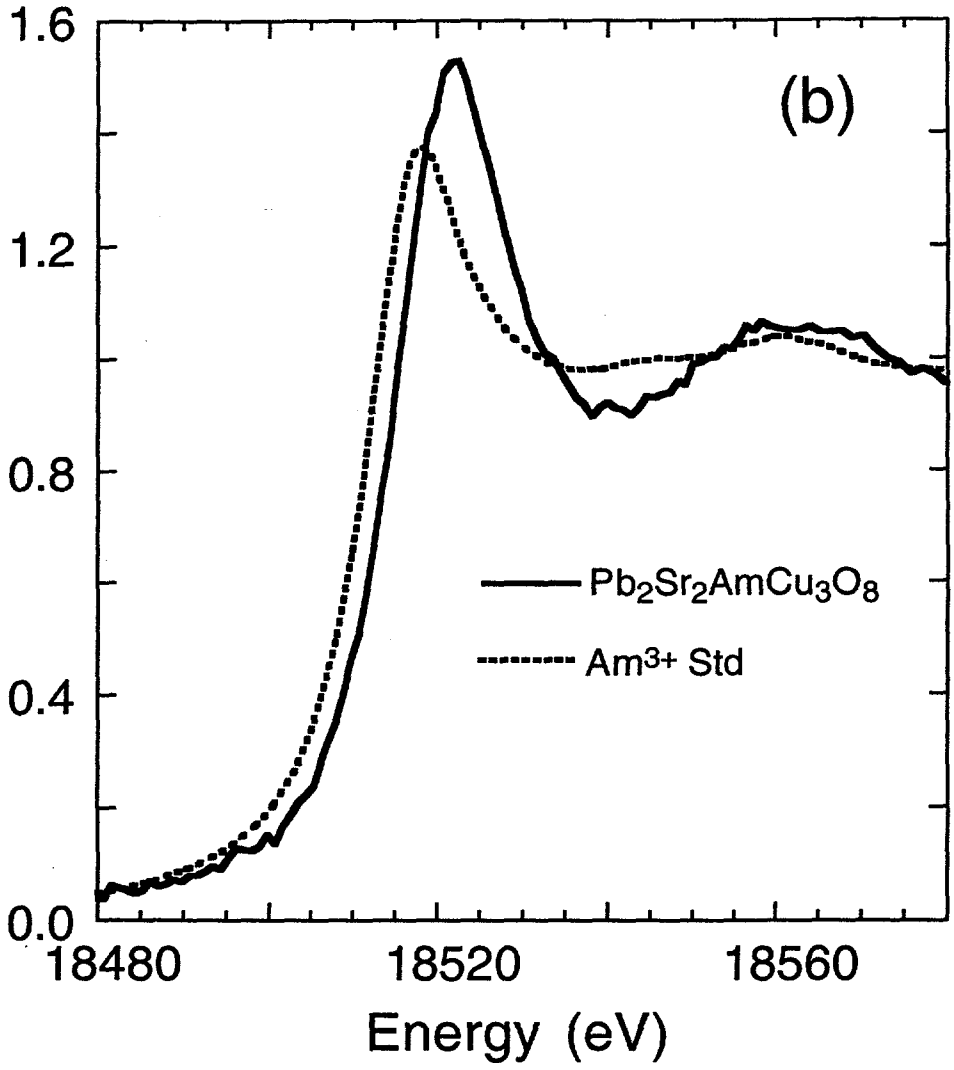

Soderholm and Staub

Figure 9b

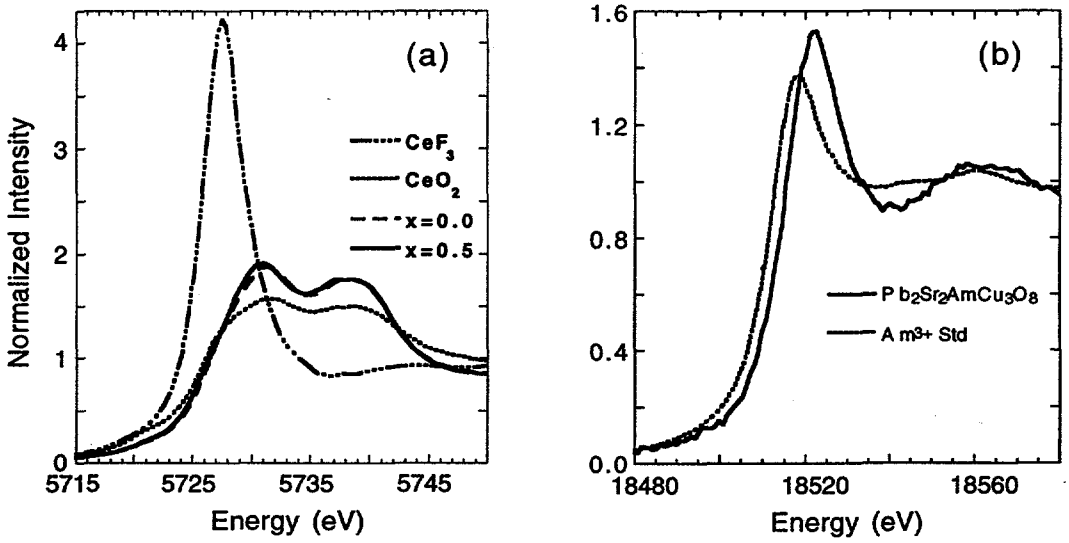

Soderholm and Staub

Figure 9 layout

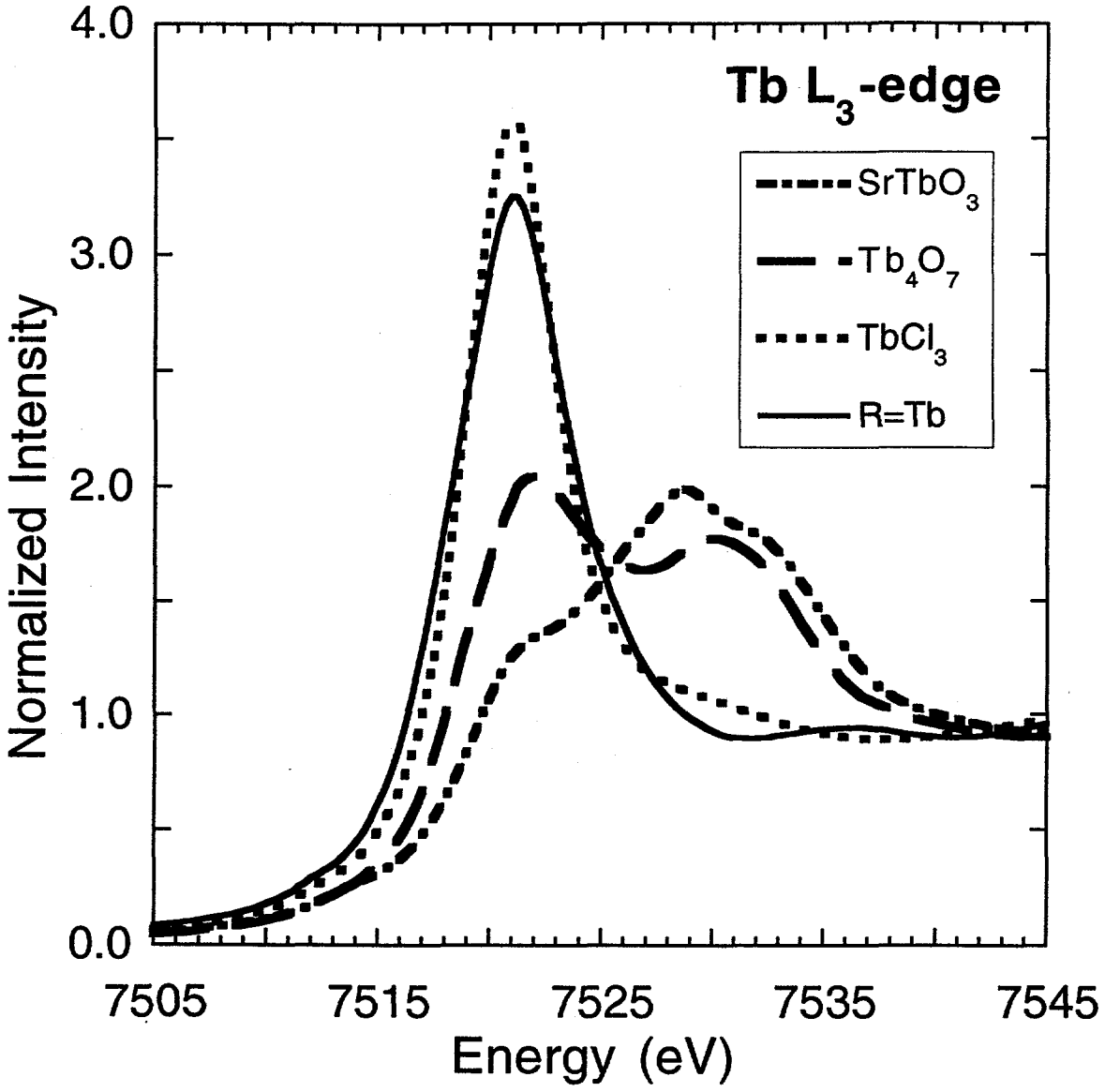

Soderholm and Staub
Figure 10

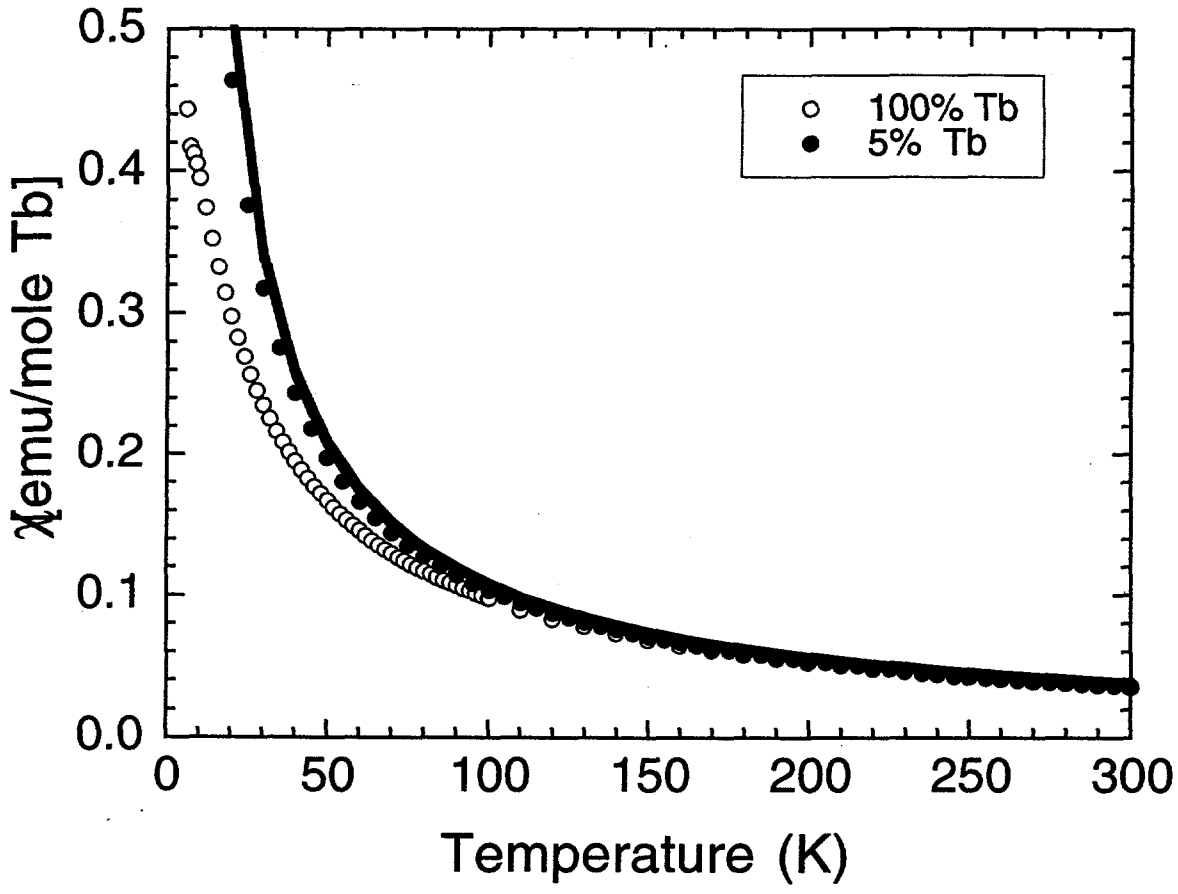

Soderholm and Staub
Figure 11

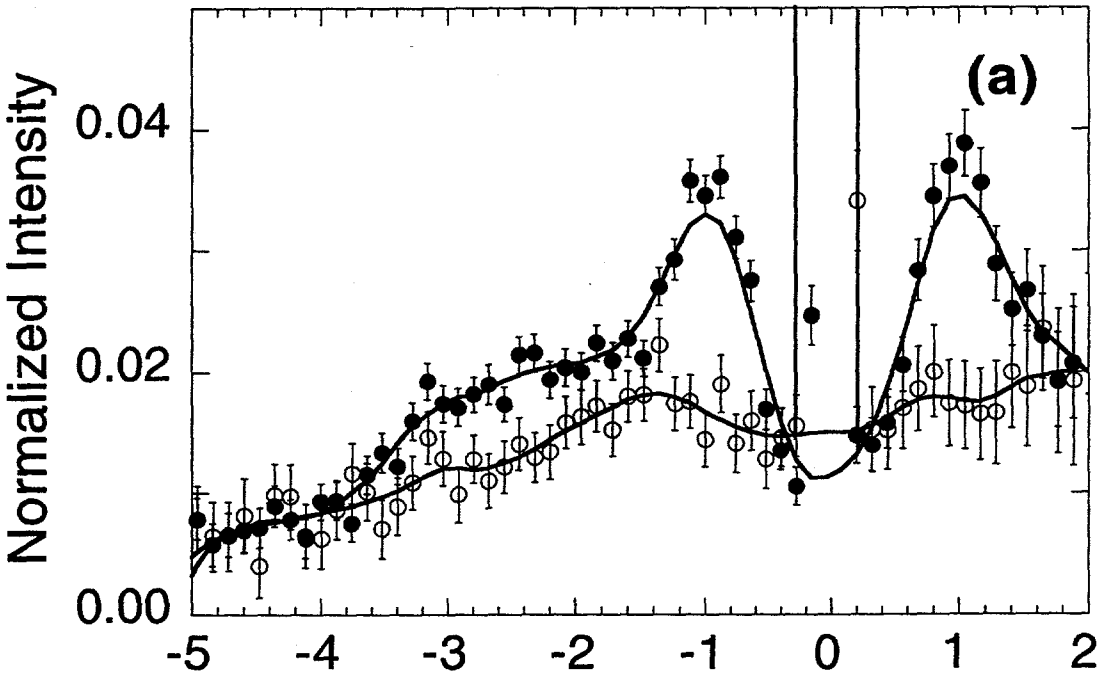

Soderholm and Staub
Figure 12 a

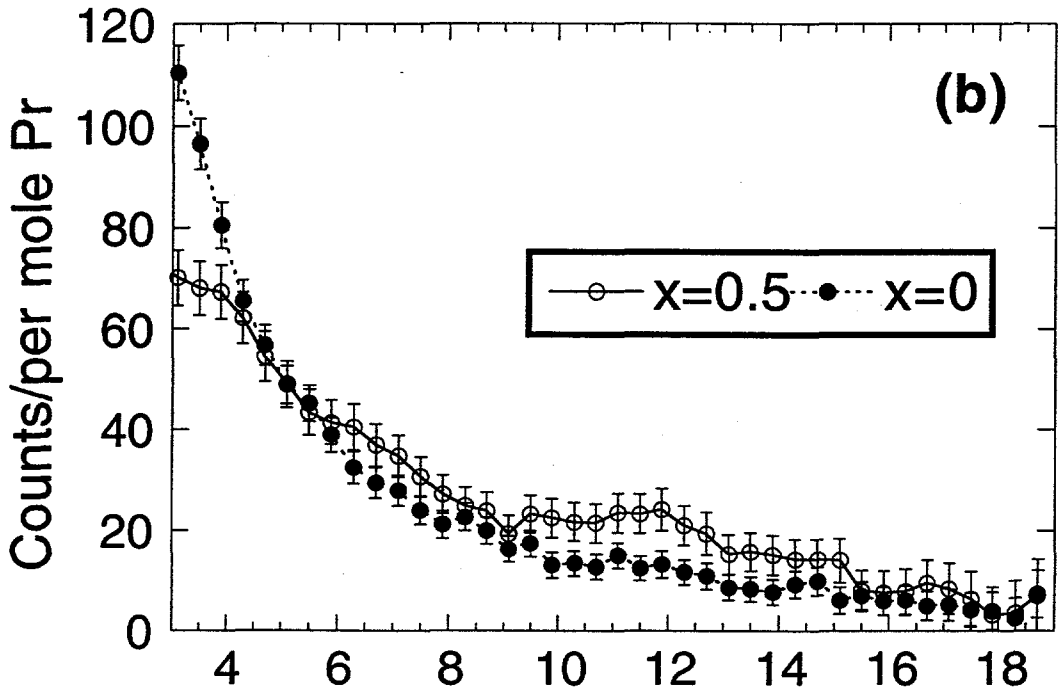

Soderholm and Staub
Figure 12b.

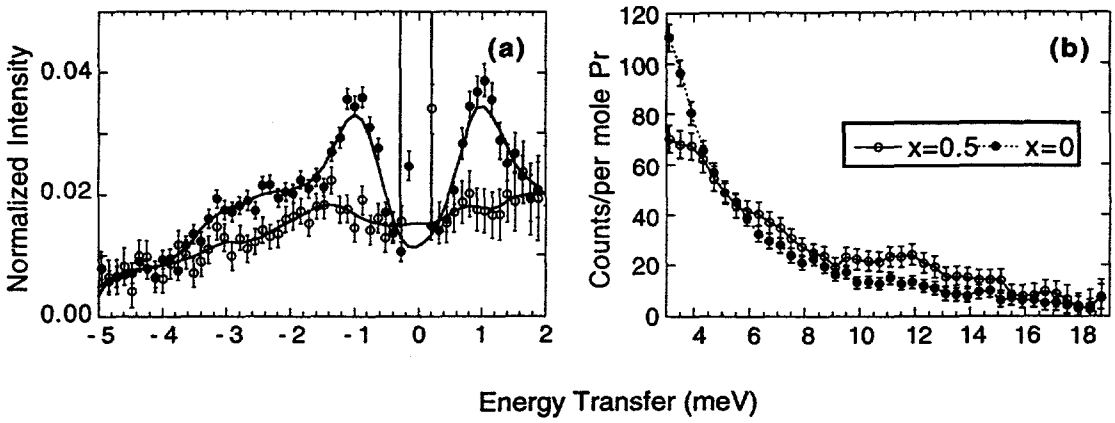

Soderholm and Staub

Figure 12 a and b layout